

## HOW RECEPTOR SURFACE DIFFUSION AND CELL ROTATION INCREASE ASSOCIATION RATES\*

SEAN D. LAWLEY<sup>†</sup> AND CHRISTOPHER E. MILES<sup>†</sup>

**Abstract.** Many biological processes are initiated when diffusing extracellular reactants reach receptors on a cell membrane. Calculating this arrival rate has therefore attracted theoretical interest for decades. However, previous work has largely ignored the fact that receptors diffuse on the two-dimensional cell membrane in a process called surface or lateral diffusion. In this work, we derive an analytical formula for this arrival rate that takes into account receptor surface diffusion and cell rotational diffusion. Our theory predicts that the impact of these diffusive processes can be quantitatively described in terms of the relative size of the cell and the reactant. As applications, our theory predicts that surface and rotational diffusion have a negligible impact on bacterial chemoreception and a moderate impact on bacteriophage adsorption. Mathematically, our model is a three-dimensional anisotropic diffusion equation coupled to boundary conditions that are described by stochastic differential equations. We first apply matched asymptotic analysis to this stochastic partial differential equation and then use probabilistic methods to show that the solution can be represented by a Brownian particle in a stochastic environment. This representation enables efficient numerical computation of solution statistics and validation of our analytical results.

**Key words.** reaction rates, lateral diffusion, asymptotic analysis, stochastic PDE

**AMS subject classifications.** 92C05, 35R60, 60H15, 35B25, 35C20

**DOI.** 10.1137/18M1217188

**1. Introduction.** Diffusion determines the timescale of many processes in both molecular and cellular biology [48]. For example, the response of cells to external stimuli often depends on the arrival of diffusing ligands to small membrane-bound receptors. Berg and Purcell calculated this arrival rate in their classic 1977 work [11], and their landmark paper has gone on to impact diverse areas of biology, including chemotaxis [15, 36, 38], regulation of gene expression [88], embryonic development [44], cell mating [72], cell division [45, 49, 51], and cell signaling [15, 88]. Remarkably, their 41-year-old paper continues to influence current research in biology [5, 41, 67].

A key result of Berg and Purcell is that the rate that extracellular ligands reach cell surface receptors can be nearly maximal, even if only a small fraction of the cell's surface contains receptors. This counterintuitive result follows from fundamental properties of diffusion. Specifically, the translational diffusion of the ligand and the cell ensures that any ligand that hits the cell surface once will in fact hit the cell surface many times and thus explore a region of the surface before diffusing away.

However, this classic work ignores two additional diffusive processes: (i) the surface diffusion of membrane-bound receptors and (ii) the rotational diffusion of the cell. That is, in addition to the three-dimensional translational diffusion of the ligand and the cell, each receptor diffuses on the two-dimensional cell surface, and the cell

---

\*Received by the editors September 27, 2018; accepted for publication (in revised form) April 29, 2019; published electronically June 20, 2019.

<http://www.siam.org/journals/siap/79-3/M121718.html>

**Funding:** This work was supported by the Center for High Performance Computing at the University of Utah. The work of the first author was supported by the National Science Foundation under grants DMS-1814832 and DMS-1148230. The work of the second author was supported by the National Science Foundation under grant DMS-1515130.

<sup>†</sup>Department of Mathematics, University of Utah, Salt Lake City, UT 84112 (lawley@math.utah.edu, miles@math.utah.edu).

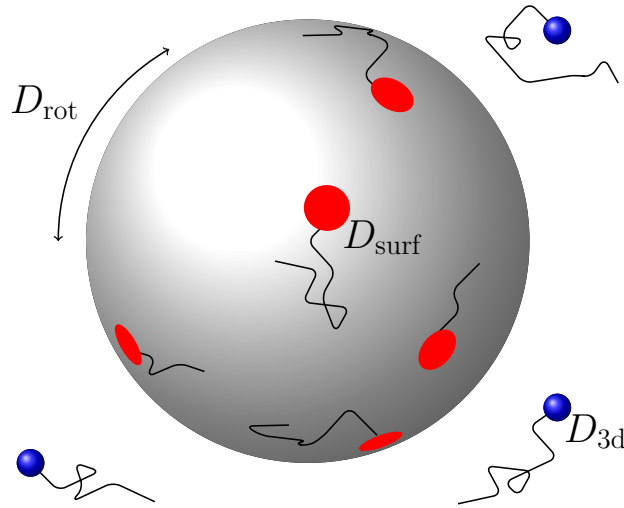


FIG. 1. Model schematic. The cell (large gray sphere) and the extracellular reactants (blue spheres) undergo translational diffusion with combined diffusivity  $D_{3d}$ . In addition, the cell surface contains  $N$  receptors (red disks) that diffuse with diffusivity  $D_{surf}$ , and the cell undergoes rotational diffusion with diffusivity  $D_{rot}$ .

undergoes rotational diffusion; see Figure 1. Receptor surface diffusion (also called “lateral” or “membrane” diffusion) is known to play a key role in certain biological processes [31, 35, 77]. More broadly, determining how features of the cell membrane affect cell signaling has been studied intensely [52]. Nevertheless, how receptor surface diffusion affects rates of binding to extracellular reactants is largely unknown. In addition, the role of rotational diffusion in association has been studied for many years [84, 13, 54]. However, theoretical studies have typically either (a) relied on computer simulations [71, 96, 37] or (b) considered the restricted case of a single receptor and employed heuristic approximations (such as the quasi-chemical approximation) to make the problem amenable to classical methods [85, 78, 12].

In this paper, we derive an analytical formula for the rate at which diffusing extracellular reactants arrive at a collection of small receptors on the surface of a cell, taking into account both receptor surface diffusion and cell rotational diffusion. After verifying our theory by computer simulations, we apply it to several biophysical scenarios. We find that the impact of surface and rotational diffusion can be described quantitatively in terms of the relative size of the cell and the reactant. As applications, our theory predicts that surface and rotational diffusion have a negligible impact on bacterial chemoreception and a moderate impact on bacteriophage adsorption. Furthermore, our results can also be applied to association rates for globular proteins, which are often modeled as spheres with small reactive sites [13, 71, 96].

Mathematically, our model consists of a three-dimensional anisotropic diffusion equation coupled to stochastically diffusing boundary conditions. More specifically, we model the extracellular reactant concentration by the diffusion equation, and the anisotropy stems from the rotational diffusion of the cell. Further, we impose an absorbing boundary condition at each of the  $N \geq 1$  cell surface receptors and a reflecting boundary condition on the rest of the cell surface. We assume that each of the  $N$  receptors diffuses on the cell surface, and thus the boundary conditions for the diffusion equation are stochastic.

We apply matched asymptotic analysis [62] to this stochastic partial differential equation (PDE) and find that reactants reach receptors at rate

$$(1) \quad J_{\max} \frac{\lambda \varepsilon N}{\lambda \varepsilon N + \pi},$$

where  $J_{\max}$  is the arrival rate to any point on the cell surface [82],  $N \geq 1$  is the number of cell surface receptors,  $\varepsilon \ll 1$  is the ratio of the radius of a receptor to the radius of the cell, and

$$\lambda := \sqrt{1 + (D_{\text{surf}} + R^2 D_{\text{rot}})/D_{3\text{d}}},$$

where  $D_{\text{surf}}$  is the surface diffusivity of each receptor,  $D_{\text{rot}}$  is the cell rotational diffusivity,  $D_{3\text{d}}$  is the sum of the translational diffusivities of the spherical cell and reactant, and  $R$  is the sum of their radii. We then show that the solution to our stochastic PDE can be represented by a certain statistic of a diffusing particle in a stochastic environment. This probabilistic representation allows us to verify (1) by particle simulation methods (as opposed to numerical solution of the time-dependent stochastic PDE).

The rest of the paper is organized as follows. In section 2, we formulate our stochastic PDE model. In section 3, we use the method of matched asymptotic expansions to analyze this stochastic PDE. In section 4, we represent the stochastic PDE solution in terms of a single Brownian particle. Relying on this probabilistic representation, we verify our asymptotic results by numerical simulations in section 5. In section 6, we apply our results to some scenarios in cell biology. We conclude by discussing related work and highlighting future directions.

**2. Model formulation.** To set up our model, we briefly review the model of Berg and Purcell [11]. Consider a spherical cell immersed in an unbounded medium containing a low concentration of spherical molecules of some reactant. Fixing our reference frame on the cell, the concentration of the reactant satisfies the diffusion equation

$$(2) \quad \partial_t c = D_{3\text{d}} \Delta c, \quad x \in \mathbb{R}^3 \setminus B_R, \quad t > 0,$$

where  $D_{3\text{d}} > 0$  is the sum of the diffusivities of the cell and the reactant, and  $\mathbb{R}^3 \setminus B_R$  is the domain exterior to the ball,

$$B_R := \{x \in \mathbb{R}^3 : |x| \leq R\},$$

where

$$R = R_{\text{cell}} + R_{\text{react}} > 0$$

is the sum of the radii of the cell and a reactant molecule. Note that (2) uses the simple geometric fact that the cell and a reactant are in contact if and only if their centers are distance  $R$  apart; see Figure 2. The concentration far from the cell is fixed,

$$(3) \quad \lim_{|x| \rightarrow \infty} c(x, t) = c_\infty > 0.$$

Assume the cell carries on its surface  $N$  receptors for the reactant. Specifically, define the spherical cap,

$$(4) \quad \Gamma(y) := \{(R_{\text{cell}}, \theta, \varphi) : (\theta - \theta_y)^2 + \sin^2(\theta_y)(\varphi - \varphi_y)^2 \leq \varepsilon^2\},$$

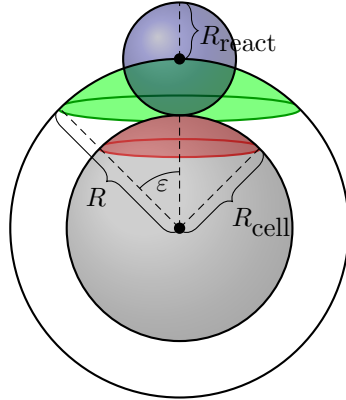


FIG. 2. A reactant molecule (blue sphere) with radius  $R_{\text{react}}$  touches a cell (gray sphere) with radius  $R_{\text{cell}}$  if and only if their centers are distance  $R = R_{\text{cell}} + R_{\text{react}}$  apart. A receptor (red region) on the cell surface is a spherical cap with angle  $\varepsilon$  (see (4)). A reactant reaches a receptor if and only if the center of the reactant reaches a spherical cap (green region) with angle  $\varepsilon$  on the sphere of radius  $R$ .

centered at a point

$$y \in \partial B_{R_{\text{cell}}} := \{x \in \mathbb{R}^3 : |x| = R_{\text{cell}}\}$$

with spherical coordinates

$$y = (R_{\text{cell}}, \theta_y, \varphi_y) \in \{R_{\text{cell}}\} \times [0, \pi) \times [0, 2\pi).$$

In the following, we make frequent use of both Cartesian and spherical coordinates.

The  $N$  receptors are then the spherical caps  $\{\Gamma(Y_n)\}_{n=1}^N$ , where

$$Y_n = (R_{\text{cell}}, \theta_n, \varphi_n)$$

is the center of the  $n$ th receptor. Notice that  $\varepsilon > 0$  is the angle between (i) the ray from the center of the cell to the apex of the cap (the pole) and (ii) the ray from the center of the cell to the edge of the disk forming the base of the cap (see Figure 2). Since the surface area of each cap is

$$\pi(\varepsilon R_{\text{cell}})^2 + \mathcal{O}(\varepsilon^3) \quad \text{for } \varepsilon \ll 1,$$

we refer to  $\varepsilon R_{\text{cell}}$  as the receptor radius.

It is easy to see from Figure 2 that a reactant molecule reaches the  $n$ th receptor  $\Gamma(Y_n)$  if and only if the center of the reactant reaches the spherical cap

$$\{(R, \theta, \varphi) : (\theta - \theta_n)^2 + \sin^2(\theta_n)(\varphi - \varphi_n)^2 \leq \varepsilon^2\} \in \partial B_R.$$

Therefore, the problem depends on the sum of radii,  $R = R_{\text{cell}} + R_{\text{react}}$ , rather than on the individual values of the cell radius,  $R_{\text{cell}}$ , and the reactant radius,  $R_{\text{react}}$ . Thus, without loss of generality, we henceforth assume that the reactants are point particles, so that  $R_{\text{react}} = 0$  and  $R_{\text{cell}} = R$ .

Any reactant molecule that touches a receptor is immediately captured by the cell, whereas reactant molecules are reflected from the cell surface between receptors. Hence, we impose absorbing boundary conditions at the receptors and reflecting

boundary conditions away from the receptors,

$$(5) \quad \begin{aligned} c &= 0, & x &\in \cup_{n=1}^N \Gamma(Y_n), \\ \partial_r c &= 0, & x &\in \partial B_R \setminus \{\cup_{n=1}^N \Gamma(Y_n)\}, \end{aligned}$$

where  $\partial_r$  denotes differentiation in the radial direction.

What is the rate that reactant molecules reach receptors? Defining this rate as the flux over the cell surface,

$$(6) \quad \lim_{t \rightarrow \infty} D_{3d} \int_{\partial B_R} \partial_r c \, dS,$$

Berg and Purcell [11] approximate the flux in (6) by the formula

$$(7) \quad J_{bp} := J_{\max} \frac{\varepsilon N}{\varepsilon N + \pi},$$

where

$$(8) \quad J_{\max} := 4\pi c_\infty D_{3d} R$$

is the flux when the entire cell surface is absorbing (the formula for  $J_{\max}$  is due to Smoluchowski [82]). The expression in (7) closely approximates (6) if both (i) the fraction of the cell surface covered by receptors is small,  $N\varepsilon^2/4 \ll 1$ , and (ii) the receptors are approximately uniformly distributed on the cell surface [62, 55].

We now generalize the model of Berg and Purcell. To determine how cell rotational diffusion affects the flux, we suppose that the cell has rotational diffusivity  $D_{\text{rot}} \geq 0$ . Allowing the reference frame to rotate with the cell effectively transfers the rotational diffusion to the reactant concentration (see [85]), so that if  $\mathbb{L}$  is the rotational Laplacian (Laplace–Beltrami) operator,

$$(9) \quad \mathbb{L} := (\sin(\theta))^{-2} \partial_{\varphi\varphi} + \cot(\theta) \partial_\theta + \partial_{\theta\theta},$$

then (2) becomes

$$(10) \quad \partial_t c = D_{3d} \Delta c + D_{\text{rot}} \mathbb{L} c, \quad x \in \mathbb{R}^3 \setminus B_R, \quad t > 0.$$

Further, to determine how receptor surface diffusion affects the flux, we suppose that the receptors diffuse independently on the cell surface with diffusivity  $D_{\text{surf}} \geq 0$ . Hence, the spherical coordinates of the center of the  $n$ th receptor now depend on time,

$$Y_n(t) = (R, \theta_n(t), \varphi_n(t)),$$

and obey the stochastic differential equations (SDEs),

$$(11) \quad \begin{aligned} d\theta_n(t) &= R^{-2} D_{\text{surf}} \cot(\theta_n(t)) \, dt + R^{-1} \sqrt{2D_{\text{surf}}} \, dW_{(\theta,n)}(t), \\ d\varphi_n(t) &= (R \sin(\theta_n(t)))^{-1} \sqrt{2D_{\text{surf}}} \, dW_{(\varphi,n)}(t), \quad n = 1, \dots, N, \end{aligned}$$

where  $\{W_{(\theta,n)}\}_{n=1}^N$  and  $\{W_{(\varphi,n)}\}_{n=1}^N$  are independent standard Brownian motions. We assume the random initial receptor positions are independent and uniformly distributed on the cell surface  $\partial B_R$ .

Hence, the receptors  $\{\Gamma(Y_n(t))\}_{n=1}^N$  now move stochastically in time and the boundary conditions in (5) become

$$(12) \quad \begin{aligned} c &= 0, & x &\in \cup_{n=1}^N \Gamma(Y_n(t)), \\ \partial_r c &= 0, & x &\in \partial B_R \setminus \{\cup_{n=1}^N \Gamma(Y_n(t))\}. \end{aligned}$$

Thus, the concentration,  $c(x, t)$ , is now a stochastic process. In the next section, we use formal asymptotic methods to analyze this stochastic PDE in the limit that the receptors are small ( $\varepsilon \ll 1$ ).

**3. Matched asymptotic analysis of the stochastic PDE.** We are interested in the large time mean flux,

$$(13) \quad J := \lim_{t \rightarrow \infty} D_{3d} \mathbb{E} \int_{\partial B_R} \partial_r c \, dS,$$

of the stochastic solution,  $c(x, t)$ , to (10)–(12). Integrating  $c(x, t)$  over the annular region  $B_{R'} \setminus B_R$  with  $R' > R$ , differentiating with respect to time, interchanging differentiation and integration, and using the divergence theorem yields

$$(14) \quad \begin{aligned} \frac{d}{dt} \int_{B_{R'} \setminus B_R} c \, dx &= D_{3d} \int_{B_{R'} \setminus B_R} \Delta c \, dx + D_{\text{rot}} \int_{B_{R'} \setminus B_R} \mathbb{L}c \, dx \\ &= D_{3d} \left( \int_{\partial B_{R'}} \partial_r c \, dS - \int_{\partial B_R} \partial_r c \, dS \right). \end{aligned}$$

In (14), we have used that

$$\mathbb{L}c = \nabla \cdot \left( 0, r \partial_\theta c, \frac{r}{\sin \theta} \partial_\varphi c \right),$$

and thus the divergence theorem ensures

$$\int_{B_{R'} \setminus B_R} \mathbb{L}c \, dx = 0.$$

Assuming

$$\lim_{t \rightarrow \infty} \mathbb{E} \frac{d}{dt} \int_{B_{R'} \setminus B_R} c(x, t) \, dx = 0,$$

it then follows from (14) that

$$\lim_{t \rightarrow \infty} \mathbb{E} \int_{\partial B_{R'}} \partial_r c \, dS = \lim_{t \rightarrow \infty} \mathbb{E} \int_{\partial B_R} \partial_r c \, dS.$$

That is, the flux across a ball of radius  $R' > R$  is independent of  $R'$ . Interchanging expectation, integration, and differentiation, we conclude

$$(15) \quad \lim_{t \rightarrow \infty} \mathbb{E}[c(x, t)] = c_\infty (1 - C|x|^{-1})$$

for some constant  $C > 0$ . In an analogy to electrostatics, we refer to  $C$  as the capacitance. Calculating the flux in (13) reduces to finding the capacitance, since (15) implies

$$(16) \quad J = 4\pi c_\infty D_{3d} C.$$

As in [11], we assume the receptors are small,  $\varepsilon \ll 1$ . For ease, we also assume that the initial concentration is given by the right-hand side of (15),

$$c(x, 0) = c_\infty(1 - C|x|^{-1}),$$

so that the mean concentration,  $\mathbb{E}[c(x, t)]$ , is constant in time. Then, if we rescale the concentration,

$$v(x, t) := \frac{-c(x, t)}{c_\infty C},$$

it follows that

$$(17) \quad \mathbb{E}[v(x, t)] = -C^{-1} + |x|^{-1} \quad \text{for all } t \geq 0.$$

We expect that  $v(x, t)$  has a boundary layer near each diffusing receptor, so we use the method of matched asymptotic expansions as in [62]. Since we expect  $C = \mathcal{O}(\varepsilon)$  [11], we expand  $v$  in the outer region away from the diffusing receptors as

$$v \sim \varepsilon^{-1}v_0 + v_1 + \dots,$$

where  $v_0$  is some constant. Substituting this outer expansion into (10)–(12) yields

$$(18) \quad \begin{aligned} \partial_t v_1 &= D_{3d}\Delta v_1 + D_{\text{rot}}\mathbb{L}v_1, & x \in \mathbb{R}^3 \setminus B_R, \\ \partial_r v_1 &= 0, & x \in \partial B_R \setminus \{\cup_{n=1}^N Y_n(t)\}. \end{aligned}$$

Observe that from the perspective of the outer solution  $v_1$ , the receptors are points. The analysis below yields the singular behavior of  $v_1$  as  $x \rightarrow Y_n(t)$ .

In the inner region near the  $n$ th receptor, we introduce the local coordinates  $(\eta, s_1, s_2)$  defined by

$$\begin{aligned} \eta &= \varepsilon^{-1}(r/R - 1), \\ s_1 &= \varepsilon^{-1} \sin(\theta_n(t))\lambda^{-1}(\varphi - \varphi_n(t)), \\ s_2 &= \varepsilon^{-1}\lambda^{-1}(\theta - \theta_n(t)), \end{aligned}$$

and define the inner solution  $w$  as a function of local coordinates,

$$(19) \quad w(\eta, s_1, s_2, t) := v(R + \varepsilon R\eta, \varphi_n(t) + \varepsilon\lambda(\sin \theta_n(t))^{-1}s_1, \theta_n(t) + \varepsilon\lambda s_2, t),$$

where

$$\lambda := \sqrt{1 + D_{2d}/D_{3d}} \quad \text{and} \quad D_{2d} := D_{\text{surf}} + R^2 D_{\text{rot}}.$$

Note that the coordinates  $(\eta, s_1, s_2)$  and the inner solution  $w$  depend on the index  $n \in \{1, \dots, N\}$ , but we have suppressed this dependence for clarity.

Assuming the function  $v(r, \theta, \varphi, t)$  is twice continuously differentiable, then a direct application of Itô’s formula [50] implies that the inner solution  $w$  satisfies the stochastic integral equation for each  $T \geq 0$ ,

$$(20) \quad \begin{aligned} w(\eta, s_1, s_2, T) - w(\eta, s_1, s_2, 0) &= \int_0^T \partial_\varphi v \, d(\varphi_n(t) + \varepsilon\lambda(\sin \theta_n(t))^{-1}s_1) \\ &+ \int_0^T \partial_\theta v \, d(\theta_n(t) + \varepsilon\lambda s_2) + \int_0^T \partial_t v \, dt \\ &+ \frac{1}{2} \int_0^T \partial_{\varphi\varphi} v \, (d(\varphi_n(t) + \varepsilon\lambda(\sin \theta_n(t))^{-1}s_1))^2 \\ &+ \frac{1}{2} \int_0^T \partial_{\theta\theta} v \, (d(\theta_n(t) + \varepsilon\lambda s_2))^2. \end{aligned}$$

We note that in the right-hand side of (20), every instance of  $v$  is evaluated at

$$v = v(R + \varepsilon R\eta, \varphi_n(t) + \varepsilon\lambda(\sin \theta_n(t))^{-1}s_1, \theta_n(t) + \varepsilon\lambda s_2, t),$$

but we have suppressed this dependence for clarity. Using the Itô calculus rules [50],

$$dW_i(t) \cdot dW_i(t) = dt, \quad dW_i(t) \cdot dW_j(t) = dW_i(t) \cdot dt = dt \cdot dt = 0 \quad \text{if } i \neq j,$$

for independent standard Brownian motions  $W_i(t)$  and  $W_j(t)$ , and the scalings,

$$\partial_r = \varepsilon^{-1}R^{-1}\partial_\eta, \quad \partial_\varphi = -\varepsilon^{-1}\lambda^{-1}\sin \theta_n(t)\partial_{s_1}, \quad \partial_\theta = -\varepsilon^{-1}\lambda^{-1}\partial_{s_2},$$

we have that (20) becomes for  $\varepsilon \ll 1$ ,

$$\begin{aligned} w(\eta, s_1, s_2, T) - w(\eta, s_1, s_2, 0) &= \varepsilon^{-2}\lambda^{-2}D_{\text{surf}}R^{-2} \int_0^T (\partial_{s_1s_1} + \partial_{s_2s_2})w \, dt \\ &\quad + \int_0^T (D_{3d}\Delta + D_{\text{rot}}\mathbb{L})v \, dt + \mathcal{O}(\varepsilon^{-1}). \end{aligned}$$

Now, it is straightforward to check that

$$\begin{aligned} D_{3d}\Delta + D_{\text{rot}}\mathbb{L} &= \varepsilon^{-2}R^{-2}D_{3d}\partial_{\eta\eta} \\ &\quad + \varepsilon^{-2}R^{-2}\lambda^{-2}(D_{3d} + R^2D_{\text{rot}})(\partial_{s_1s_1} + \partial_{s_2s_2}) + \mathcal{O}(\varepsilon^{-1}). \end{aligned}$$

Hence, using the definition of  $\lambda$  and  $w$ , we have that

$$(21) \quad w(\eta, s_1, s_2, T) - w(\eta, s_1, s_2, 0) = \varepsilon^{-2}R^{-2}D_{3d} \int_0^T (\partial_{\eta\eta} + \partial_{s_1s_1} + \partial_{s_2s_2})w \, dt + \mathcal{O}(\varepsilon^{-1}).$$

Plugging the inner expansion  $w = \varepsilon^{-1}w_0 + w_1 + \dots$  into (21) and using that  $T \geq 0$  is arbitrary implies that  $w_0$  is harmonic in the upper half-space,

$$(22) \quad (\partial_{\eta\eta} + \partial_{s_1s_1} + \partial_{s_2s_2})w_0 = 0, \quad \eta > 0, \quad s_1 \in \mathbb{R}, \quad s_2 \in \mathbb{R}.$$

Furthermore, it follows immediately from the definition of  $v$  and  $w$  that  $w_0$  satisfies the following boundary conditions on the  $\eta = 0$  plane,

$$\begin{aligned} \partial_\eta w_0 &= 0 \quad \text{on } \eta = 0, \quad s_1^2 + s_2^2 \geq \lambda^{-2}, \\ w_0 &= 0 \quad \text{on } \eta = 0, \quad s_1^2 + s_2^2 \leq \lambda^{-2}. \end{aligned}$$

This problem for  $w_0$  can be solved using the solution to the so-called electrified disk problem from electrostatics [40]. Explicitly, we have that

$$w_0 = A(1 - (2/\pi) \arcsin(\zeta)),$$

where

$$\zeta := 2\left([\sigma + 1]^2 + \eta^2\right)^{1/2} + \left([\sigma - 1]^2 + \eta^2\right)^{1/2} \quad \text{and} \quad \sigma := \sqrt{s_1^2 + s_2^2},$$

and thus  $w_0$  has the far-field behavior

$$(23) \quad w_0 \sim A(1 - 2(\lambda\pi\rho)^{-1}) \quad \text{as } \rho := \sqrt{\eta^2 + s_1^2 + s_2^2} \rightarrow \infty,$$

where  $A$  is a constant to be determined by matching to the outer solution.

The matching condition is that the near-field behavior of the outer expansion as  $x \rightarrow Y_n(t)$  must agree with the far-field behavior of the inner expansion as  $\rho \rightarrow \infty$ . That is,

$$(24) \quad \varepsilon^{-1}v_0 + v_1 + \dots \sim \varepsilon^{-1}w_0 + w_1 + \dots \quad \text{as } x \rightarrow Y_n(t), \rho \rightarrow \infty.$$

Plugging (23) into (24) implies that  $A = v_0$  and that  $v_1$  has the following singular behavior,

$$(25) \quad v_1 \sim \frac{-v_0 2/\pi}{\sqrt{\lambda^2(\frac{r}{R} - 1)^2 + \sin^2(\theta_n(t))(\varphi - \varphi_n(t))^2 + (\theta - \theta_n(t))^2}} \quad \text{as } x \rightarrow Y_n(t).$$

Writing the singular behavior in (25) in distributional form, the problem in (18) becomes

$$(26) \quad \partial_t v_1 = D_{3d} \Delta v_1 + D_{\text{rot}} \mathbb{L} v_1, \quad x \in \mathbb{R}^3 \setminus B_R,$$

$$(27) \quad \partial_r v_1 = \frac{4\lambda v_0}{R} \sum_{n=1}^N \frac{\delta(\theta - \theta_n(t))}{\sin(\theta_n(t))} \delta(\varphi - \varphi_n(t)), \quad x \in \partial B_R.$$

To see why (26)–(27) is the distributional form of (18) and (25), suppose a function  $f$  satisfies (26)–(27). To determine the behavior of  $f$  as  $x \rightarrow Y_n(t) \in \partial B_R$ , let  $0 < \bar{\varepsilon} \ll 1$  and define (analogously to (19))

$$g(\bar{\eta}, \bar{s}_1, \bar{s}_2, t) := f(R + \bar{\varepsilon} R \bar{\eta}, \varphi_n(t) + \bar{\varepsilon} \lambda (\sin \theta_n(t))^{-1} \bar{s}_1, \theta_n(t) + \bar{\varepsilon} \lambda \bar{s}_2, t),$$

for  $\bar{\eta} > 0$ ,  $\bar{s}_1 \in \mathbb{R}$ ,  $\bar{s}_2 \in \mathbb{R}$ . Expanding  $g$  as  $g = g_0/\bar{\varepsilon} + g_1 + \dots$ , the argument that led to (22) yields that  $g_0$  satisfies

$$(28) \quad (\partial_{\bar{\eta}\bar{\eta}} + \partial_{\bar{s}_1\bar{s}_1} + \partial_{\bar{s}_2\bar{s}_2})g_0 = 0, \quad \bar{\eta} > 0, \bar{s}_1 \in \mathbb{R}, \bar{s}_2 \in \mathbb{R}.$$

Furthermore, a direct calculation using (27) shows that

$$\partial_{\bar{\eta}} g(\bar{\eta}, \bar{s}_1, \bar{s}_2, t) = \frac{4v_0}{\lambda \bar{\varepsilon}} \delta(\bar{s}_1) \delta(\bar{s}_2)$$

and, thus,

$$(29) \quad \partial_{\bar{\eta}} g_0 = \frac{4v_0}{\lambda} \delta(\bar{s}_1) \delta(\bar{s}_2), \quad \bar{\eta} = 0, \bar{s}_1 \in \mathbb{R}, \bar{s}_2 \in \mathbb{R}.$$

The solution to (28) and (29) is

$$g_0 = \frac{-2v_0}{\lambda \pi \sqrt{\bar{\eta}^2 + \bar{s}_1^2 + \bar{s}_2^2}}.$$

Matching the far-field behavior of  $g_0/\bar{\varepsilon}$  with the near-field behavior of  $f$  implies that  $f$  has the singular behavior in (25) as  $x \rightarrow Y_n(t)$ .

As in (14) above, we integrate (26) over the annular region  $B_{R'} \setminus B_R$  with  $R' > R$  and use the divergence theorem and the boundary conditions in (27) to obtain

$$(30) \quad \begin{aligned} \frac{d}{dt} \int_{B_{R'} \setminus B_R} v_1 \, dx &= D_{3d} \int_{B_{R'} \setminus B_R} \Delta v_1 \, dx + D_{\text{rot}} \int_{B_{R'} \setminus B_R} \mathbb{L} v_1 \, dx \\ &= D_{3d} \left( \int_{\partial B_{R'}} \partial_r v_1 \, dS - \int_{\partial B_R} \partial_r v_1 \, dS \right) \\ &= D_{3d} \left( \int_{\partial B_{R'}} \partial_r v_1 \, dS - 4\lambda v_0 R N \right). \end{aligned}$$

Now, it follows from (17) that

$$\mathbb{E} \int_{\partial B_{R'}} \partial_r v_1 \, dS = -4\pi.$$

Hence, taking the expectation of (30) at large time determines the value of  $v_0$ ,

$$v_0 = \frac{-\pi}{\lambda RN}.$$

Since  $-c(x, t)/(c_\infty C) = v(x, t) \sim \varepsilon^{-1} v_0$  and  $c \rightarrow c_\infty$  as  $|x| \rightarrow \infty$ , we obtain the following asymptotic behavior of the capacitance,

$$(31) \quad C \sim \lambda \varepsilon N R / \pi \quad \text{as } \varepsilon \rightarrow 0.$$

By (16), the flux in (13) has the leading order behavior

$$(32) \quad J \sim J_{\max} \lambda \varepsilon N / \pi \quad \text{as } \varepsilon \rightarrow 0.$$

To summarize, if we compare (32) to (7), then we see that surface and rotational diffusion increase the flux by the dimensionless factor  $\lambda = \sqrt{1 + D_{2d}/D_{3d}}$  in the small receptor limit ( $\varepsilon \ll 1$ ), where  $D_{2d} = D_{\text{surf}} + R^2 D_{\text{rot}}$  is the effective two-dimensional receptor diffusivity. Since  $\lambda \geq 1$ , (32) implies that allowing the receptors to diffuse and/or allowing the cell to rotate strictly increases the flux to receptors. One way to interpret (32) is that the effective radius of each receptor is increased by  $\lambda \geq 1$ , so that the effective area of each receptor increases from  $\pi(\varepsilon R)^2$  to

$$\pi(\lambda \varepsilon R)^2 = (1 + D_{2d}/D_{3d})\pi(\varepsilon R)^2.$$

**3.1. Incorporating receptor competition.** The flux formula in (32) is valid in the small receptor limit,  $\varepsilon \rightarrow 0$ . However, the formula breaks down if we take the number of receptors  $N \rightarrow \infty$  for fixed  $\varepsilon > 0$ . To see why, observe that the receptors completely cover the cell surface if  $N \rightarrow \infty$ , and thus the flux in (13) must approach  $J_{\max}$  in (8) as  $N \rightarrow \infty$ . However, (32) grows without bound as  $N \rightarrow \infty$ . Similarly, (32) grows without bound as  $\lambda \rightarrow \infty$ .

To ameliorate this problem, we adapt the approach of [79] and homogenize the stochastic and heterogeneous boundary conditions in (12) by the Robin condition,

$$(33) \quad D_{3d} \partial_r c = \kappa c, \quad x \in \partial B_R,$$

where  $\kappa > 0$  is the so-called ‘‘leakage’’ parameter. Note that (33) becomes perfectly reflecting (perfectly absorbing) in the limit  $\kappa \rightarrow 0$  ( $\kappa \rightarrow \infty$ ).

To derive a formula for  $\kappa$ , we note that (15) implies that the large time mean of the solution to (3), (10), and (12) satisfies a Robin condition of the form of (33) with

$$\kappa = \frac{D_{3d} C}{R^2 - CR}.$$

Hence, the formula for the capacitance in (31) yields

$$(34) \quad \kappa \sim \frac{D_{3d} \lambda \varepsilon N}{\pi R} \quad \text{as } \varepsilon \rightarrow 0.$$

Now, if  $c(x, t)$  satisfies (3), (10), and (33), then its large time flux defined in (6) is

$$(35) \quad J_{\max} \frac{\kappa R}{D_{3d} + \kappa R}.$$

Plugging (34) into (35) yields the approximation

$$(36) \quad J_* := J_{\max} \frac{\lambda \varepsilon N}{\lambda \varepsilon N + \pi} \approx J := \lim_{t \rightarrow \infty} D_{3d} \mathbb{E} \int_{\partial B_R} \partial_r c \, dS.$$

**3.2. Limiting behavior of the flux.** Before verifying that  $J_*$  in (36) closely approximates  $J$  for  $\varepsilon \ll 1$  in the following sections, we first check that  $J_*$  has the desired behavior in various parameter limits. First,

$$J_* \sim J_{\max} \lambda \varepsilon N / \pi \quad \text{as } \varepsilon \rightarrow 0,$$

as required by (32). Second,  $J_*$  reduces to the Berg and Purcell flux,  $J_{\text{bp}}$ , in (7) for immobile receptors on a nonrotating cell. That is, setting  $D_{\text{surf}} = D_{\text{rot}} = 0$  implies  $\lambda = 1$  and thus  $J_*$  reduces to  $J_{\text{bp}}$ . In fact,

$$J_* \sim J_{\text{bp}} \quad \text{as } D_{2d}/D_{3d} \rightarrow 0.$$

Third, in the many receptor limit,  $J_*$  approaches the flux for a cell whose entire surface is absorbing,

$$J_* \rightarrow J_{\max} \quad \text{as } N \rightarrow \infty.$$

Finally, the most interesting limit is that of large surface and/or rotational diffusivity, in which we find

$$(37) \quad J_* \sim J_{\max} \quad \text{as } D_{2d}/D_{3d} \rightarrow \infty.$$

Curiously, (37) implies that the  $N$  receptors are effectively everywhere on the cell surface at once if  $D_{2d}/D_{3d} \gg 1$ . For example, even in the case when a very small fraction,  $f \in (0, 1)$ , of the cell surface is absorbing,

$$(38) \quad f \approx \frac{N\pi(\varepsilon R)^2}{4\pi R^2} = \frac{N\varepsilon^2}{4} \ll 1,$$

the flux can be nearly identical to the flux for a cell whose entire surface is absorbing, provided  $D_{2d}/D_{3d}$  is sufficiently large.

To understand this result, we note three facts. First, a fundamental property of diffusion ensures that any reactant that hits the cell surface once will necessarily hit the cell surface many times before diffusing away. (In fact, if a Brownian particle hits a boundary once, then the particle hits the boundary infinitely many times [50]). Second, the time between hits to the cell surface is inversely proportional to  $D_{3d}$ . Third, the equilibrium distribution of the receptors is uniform on the cell surface, and the relaxation rate to this equilibrium is proportional to  $D_{2d}$ .

Therefore, if  $D_{2d}/D_{3d} \gg 1$ , then any reactant that hits the cell surface once will hit the surface many times and the distribution of the receptors at a large subset of these hitting times will be approximately uniform and independent. Hence, even if the probability that the reactant hits a receptor upon a single hit to the cell surface is small (this probability is the fraction  $f$  in (38)), the reactant hits the cell surface many times, and the receptor distribution is independent at many of these hits, and thus the reactant hits a receptor with high probability. We note that a similar phenomenon was discovered in [60], in which a boundary that switches temporally between absorbing and reflecting becomes perfectly absorbing in the limit that the switching is fast compared to the diffusion timescale of the particles.

**4. Particle perspective of the stochastic PDE.** In this section, we show that the solution to the stochastic PDE in (10)–(12) is a certain statistic of a single particle diffusing in an environment that changes stochastically in time. This representation allows us to numerically approximate the solution of the PDE by Monte Carlo simulations of a single diffusing particle. Without this representation, we would need to numerically solve the time-dependent stochastic PDE over many realizations of the stochastic boundary conditions. Such a procedure would be quite intractable, as numerically solving the steady state PDE for stationary receptors is already a difficult problem that requires sophisticated numerical methods [14].

Consider a diffusing particle  $X(t) \in \overline{\mathbb{R}^3 \setminus B_R}$  with spherical coordinates

$$X(t) = (r(t), \Theta(t), \Phi(t)) \in [R, \infty) \times [0, \pi) \times [0, 2\pi)$$

satisfying

$$(39) \quad dr(t) = 2D_{3d}(r(t))^{-1} dt + \sqrt{2D_{3d}} dW_r(t) + dL(t),$$

$$(40) \quad d\Theta(t) = D(t) \cot(\Theta(t)) dt + \sqrt{2D(t)} dW_\Theta(t),$$

$$(41) \quad d\Phi(t) = \sqrt{2D(t)} (\sin(\Theta(t)))^{-1} dW_\Phi(t),$$

where  $W_r(t), W_\Theta(t), W_\Phi(t)$  are independent standard Brownian motions,  $D(t) := D_{3d}(r(t))^{-2} + D_{\text{rot}}$ , and  $L(t)$  is the local time of  $X(t)$  in  $\partial B_R$ . That is,  $L(t)$  is nondecreasing and increases only when  $X(t)$  is in  $\partial B_R$ . The significance of the local time term in (39) is that it forces  $X(t)$  to reflect from  $\partial B_R$  and thus ensures that  $X(t) \in \overline{\mathbb{R}^3 \setminus B_R}$  for all  $t \geq 0$  (see, for example, Chapter 6, page 399 and following in [50] for more on local time theory). We note that the dynamics of  $X(t)$  are chosen so that its infinitesimal generator involves the self-adjoint differential operator,  $D_{3d}\Delta + D_{\text{rot}}\mathbb{L}$ , on the right-hand side of (10).

For our analysis in this section, it is convenient to assume the paths of the receptors  $\mathbf{Y}(t) = (Y_1(t), \dots, Y_N(t)) \in (\partial B_R)^N$  satisfy (11) for all  $t \in \mathbb{R}$  (rather than only  $t \geq 0$ ). For  $T \geq 0$ , define the stopping time

$$(42) \quad \tau(T) := \inf\{t > 0 : X(t) \in \cup_{n=1}^N \{\Gamma(Y_n(T-t))\}\} \leq \infty,$$

which is the first time  $X(t)$  reaches one of the  $N$  diffusing receptors, where time runs in reverse for the receptors. If  $\tau = \infty$ , then the particle  $X(t)$  never reaches a diffusing receptor. Since three-dimensional Brownian motion is transient, the event  $\tau = \infty$  occurs with strictly positive probability.

In the following, let  $\mathbb{E}_x$  denote expected value conditioned on the initial location,

$$(43) \quad X(0) = x \in \overline{\mathbb{R}^3 \setminus B_R}.$$

Further, let  $\mathbb{E}_x[\cdot | \mathbf{Y}]$  denote expected value conditioned on (43) and a realization of the diffusing receptors,  $\mathbf{Y} = \{(Y_1(t), \dots, Y_N(t))\}_{t \in \mathbb{R}}$ . Similarly, let  $\mathbb{P}_x$  and  $\mathbb{P}_x(\cdot | \mathbf{Y})$  denote the associated probability measures. We emphasize that the receptors  $\mathbf{Y}$  and the particle  $X$  are independent.

For  $T \geq 0$ , define the stochastic process

$$Z(t) := c(X(t), T-t), \quad t \in [0, T],$$

where  $c(x, t)$  satisfies (10)–(12). Note that  $Z$  depends on the path of  $X$  and  $\mathbf{Y}$ .

Applying Itô's formula to  $Z(t)$  yields

$$\begin{aligned}
 (44) \quad & Z(t) - Z(0) = c(X(t), T - t) - c(X(0), T) \\
 &= \int_0^t (-\partial_t + D_{3d}\Delta + D_{\text{rot}}\mathbb{L})c(X(s), T - s) \, ds + \int_0^t \partial_r c(X(s), T - s) \, dL(s) + M \\
 &= 0 + \int_0^t \partial_r c(X(s), T - s) \, dL(s) + M,
 \end{aligned}$$

where  $M$  satisfies  $\mathbb{E}_x[M|\mathbf{Y}] = 0$ . We have used (10) in the final equality in (44).

If we evaluate (44) at  $t$  equal to the stopping time given by the minimum of  $\tau(T)$  and  $T$  and use the definition of  $\tau(T)$  in (42) and the boundary conditions in (12), then we obtain

$$(45) \quad c(X(\min\{\tau(T), T\}), T - \min\{\tau(T), T\}) - c(X(0), T) = M \quad \text{almost surely.}$$

Taking the expectation of (45) conditioned on a realization  $\mathbf{Y}$  of receptor paths yields

$$\begin{aligned}
 (46) \quad & \mathbb{E}_x[c(X(0), T) | \mathbf{Y}] = \mathbb{E}_x \left[ c(X(\min\{\tau(T), T\}), T - \min\{\tau(T), T\}) | \mathbf{Y} \right] \\
 &= \mathbb{E}_x [c(X(\tau(T)), T - \tau(T)) 1_{\tau(T) \leq T} | \mathbf{Y}] \\
 &\quad + \mathbb{E}_x [c(X(T), 0) 1_{\tau(T) > T} | \mathbf{Y}],
 \end{aligned}$$

where  $1_A$  denotes the indicator function on an event  $A$ , which is defined to be 1 if  $A$  occurs and 0 otherwise. Now,  $c(x, T)$  is measurable with respect to  $\mathbf{Y}$  and, therefore,

$$(47) \quad \mathbb{E}_x [c(X(0), T) | \mathbf{Y}] = c(x, T).$$

Further, by the definition of  $\tau(T)$  in (42) and the boundary conditions in (12), we have that

$$(48) \quad c(X(\tau(T)), T - \tau(T)) 1_{\tau(T) \leq T} = 0 \quad \text{almost surely.}$$

Hence, if we assume the initial condition

$$c(x, 0) = c_\infty, \quad x \in \mathbb{R}^3 \setminus B_R,$$

then (46)–(48) yield

$$(49) \quad c(x, T) = c_\infty \mathbb{P}_x(\tau(T) > T | \mathbf{Y}) \quad \text{for } T \geq 0 \text{ almost surely.}$$

Equation (49) highlights that there are two sources of randomness in this model. Namely, there is the random path of the particle,  $X$ , and the random paths of the receptors,  $\mathbf{Y}$ . Equation (49) (and thus (10)–(12)) is an average over particle paths for a fixed realization of the receptor paths. Therefore, (49) depends on the realization of receptor paths,  $\mathbf{Y}$ .

If we take the expectation of (49) over receptor paths, then we obtain

$$(50) \quad \mathbb{E}[c(x, T)] = c_\infty \mathbb{P}_x(\tau > T),$$

where we have defined  $\tau := \tau(0)$ , since the stationarity of the receptor distribution and the independence of  $X$  and  $\mathbf{Y}$  ensure that

$$\mathbb{P}_x(\tau(s) > T) = \mathbb{P}_x(\tau(t) > T) \quad \text{for all } s, t \in \mathbb{R}.$$

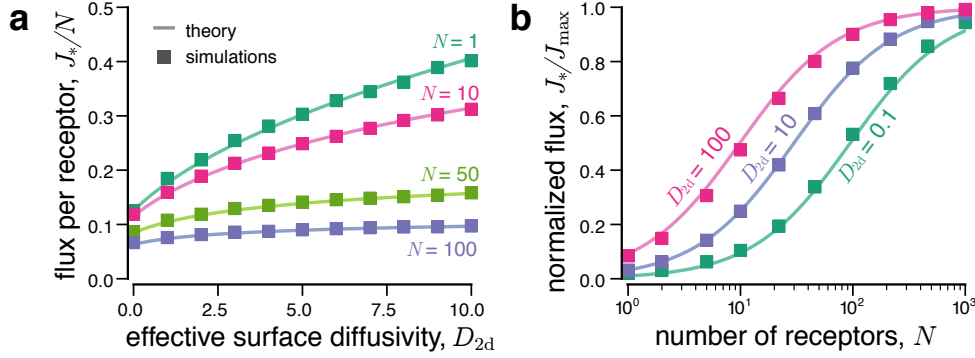


FIG. 3. Theory and numerical simulations. a: Flux per receptor as a function of surface and rotational diffusivity  $D_{2d} := D_{\text{surf}} + R^2 D_{\text{rot}}$  for different numbers of receptors,  $N$ . The curves are  $J_*/N$  for  $J_*$  in (36). b: Normalized reaction rate as a function  $N$  for different values of  $D_{2d}$ . The curves are  $J_*/J_{\max}$  for  $J_*$  in (36). In both plots,  $\varepsilon = 10^{-1.5} \approx 0.03$  and  $R = D_{3d} = 1$ . See the text for simulation details.

Taking  $T \rightarrow \infty$  in (50) yields

$$(51) \quad \lim_{T \rightarrow \infty} \mathbb{E}[c(x, T)] = c_\infty \mathbb{P}_x(\tau = \infty) = c_\infty (1 - C|x|^{-1}).$$

In words, (51) states that the large time mean of the stochastic PDE in (10)–(12) evaluated at a point  $x \in \mathbb{R}^3 \setminus B_R$  is the far-field concentration  $c_\infty$  multiplied by the probability that a particle starting at  $x \in \mathbb{R}^3 \setminus B_R$  will escape to spatial infinity rather than be absorbed at a diffusing receptor. We note that the escape probability of a single diffusing particle is often used to study association rates [2, 95].

**5. Numerical simulation.** The relation in (51) allows us to numerically estimate the large time mean of the stochastic PDE in (10)–(12) by simulating the diffusive path of a particle in the presence of diffusing receptors. Before detailing our simulation method, we outline the main points. We simulate the path of a single particle diffusing outside the cell and the paths of diffusing cell surface receptors until the particle either reaches a receptor or reaches some large outer radius  $R_\infty \in (R, \infty)$ . We then repeat this process many times and compute the fraction of particles that reach the outer radius before reaching a receptor. A certain modification of this fraction then yields an approximation to the probability that the particle escapes to spatial infinity,  $\mathbb{P}_x(\tau = \infty)$ . Equation (51) then relates this probability to the capacitance  $C$  of the large time mean solution, which in turn yields the mean flux by (16).

Figure 3 shows excellent agreement between these stochastic simulations and our analytical formula  $J_*$  in (36) for the flux. The largest error is in Figure 3(b) when  $D_{2d} = 0.1$  and  $N = 1000$ , in which case the surface area fraction,  $f \in (0, 1)$ , covered by receptors is  $f \approx N\varepsilon^2/4 = 1/4$ . This error is to be expected, since our approximation  $J_*$  reduces to the Berg–Purcell approximation  $J_{\text{bp}}$  when  $D_{2d} = 0$ , and it is known that the accuracy of  $J_{\text{bp}}$  breaks down if  $f$  is not sufficiently small [62, 55]. We also note that the accuracy of  $J_{\text{bp}}$  requires an approximate uniform arrangement of well-separated receptors [62, 55]. If the receptors diffuse independently, then their distribution converges exponentially in time to a random uniform distribution on the surface, regardless of their initial placement. Hence, if the expected area fraction is small,  $f \ll 1$ , then receptor diffusion ensures that receptors will be uniformly distributed and well-separated with high probability.

We now describe our stochastic simulation algorithm in more detail. For  $R = D_{3d} = 1$ ,  $\varepsilon = 10^{-1.5} \approx 0.03$ , and varying values of  $D_{2d}$  and  $N$ , we simulated the diffusive paths of  $10^5$  particles satisfying the SDEs (39)–(41). For each of the  $10^5$  particles, we also simulated the paths of the  $N$  surface receptors satisfying (11). We used the Euler–Maruyama method [53] for both the particle and receptor paths. The simulation data plotted in Figure 3 is for  $D_{\text{surf}} = D_{\text{rot}} = \frac{1}{2}D_{2d}$ , though we found that simulation data for both  $D_{\text{surf}} = D_{2d}, D_{\text{rot}} = 0$  and  $D_{\text{rot}} = D_{2d}, D_{\text{surf}} = 0$  were indistinguishable (as predicted by (36)).

Initially, we place the particle at radius  $R_0 \in (R, R_\infty)$  (we take  $R_0 = 1.1$ ) and randomly distribute the receptors uniformly on the sphere. The discrete time step  $\Delta t$  for the Euler–Maruyama method varied between  $10^{-4}$  and  $10^{-2}$ , depending on the radial distance away from either boundary. That is,  $\Delta t$  transitions from small to large by a heuristically determined sigmoidal function of  $\min\{r - R, R_\infty - r\}$ . When the particle hits the cell surface, it is either absorbed if it hits a receptor or reflected off the sphere using the tangent plane at the point of intersection. Each simulation runs until the particle is absorbed at either a receptor or the large outer radius  $R_\infty$  (we take  $R_\infty = 10$ ). To determine if the particle is absorbed at the outer radius during a given time step, we first note that if the radius of the particle at the end of the time step is larger than  $R_\infty$ , then the particle should obviously be absorbed. However, it is also possible for the particle to be absorbed at  $R_\infty$  if the radius of the particle is less than  $R_\infty$  at both the start and the end of a time step. Neglecting curvature and following [4], the probability of crossing  $R_\infty$  in a time step initially distance  $\ell_i$  from  $R_\infty$  and updated to distance  $\ell_u$  is given by  $\exp(-2\ell_i\ell_u/s^2)$ , where  $s := \sqrt{2D_{3d}\Delta t}$ .

For a set of  $10^5$  trials with fraction  $q \in [0, 1]$  absorbed at  $R_\infty$ , we obtain the approximation

$$(52) \quad q \approx \mathbb{P}_{R_0}(\tau > \tau_{R_\infty}),$$

where  $\mathbb{P}_r$  is the probability measure conditioned on an initial particle radius,  $|X(0)| = r$ , and  $\tau_{R_\infty}$  is the first time the particle reaches the outer radius  $R_\infty$ ,

$$\tau_{R_\infty} := \inf\{t > 0 : |X(t)| = R_\infty\}.$$

To find an approximation for  $\mathbb{P}_{R_0}(\tau = \infty)$ , we follow [69, 70] and note that

$$(53) \quad 1 - \frac{C}{R_0} = \mathbb{P}_{R_0}(\tau = \infty) = \mathbb{P}_{R_0}(\tau = \infty \mid \tau > \tau_{R_\infty})\mathbb{P}_{R_0}(\tau > \tau_{R_\infty}) \\ \approx \mathbb{P}_{R_\infty}(\tau = \infty)\mathbb{P}_{R_0}(\tau > \tau_{R_\infty}) = \left(1 - \frac{C}{R_\infty}\right)\mathbb{P}_{R_0}(\tau > \tau_{R_\infty}).$$

The error in the approximate equality (53) vanishes as  $R_\infty/R$  and/or  $D_{2d}/D_{3d}$  grow. Rearranging (53) and using (52) yields a numerical approximation to the capacitance,

$$C \approx \frac{(1 - q)R_0R_\infty}{R_\infty - qR_0}.$$

Plugging this value into (16) yields our numerical approximation to the flux that is plotted in Figure 3 against our asymptotic formula for the flux in (36).

**6. Applications to cell biology.** Summarizing (32), an extracellular reactant diffusing with diffusivity  $D_{3d}$  reaches a small surface-bound receptor at rate

$$(54) \quad k := \lambda k_0 \quad \text{with } \lambda := \sqrt{1 + D_{2d}/D_{3d}},$$

where  $D_{2d} := D_{\text{surf}} + R^2 D_{\text{rot}}$  is the sum of the receptor surface diffusivity and the cell rotational diffusivity, and  $k_0$  is the corresponding rate for an immobile receptor ( $D_{\text{surf}} = 0$ ) on a nonrotating cell ( $D_{\text{rot}} = 0$ ). That is, surface and rotational diffusion increase the “reaction” rate by the factor  $\lambda \geq 1$ . As previous rate calculations have largely omitted surface and rotational diffusion, we now investigate when such an omission is valid.

**6.1. General biophysical calculations.** Before discussing (54) in some specific biological contexts, we perform some general calculations based on the relative sizes of the cell and the reactant that is to bind to a cell receptor. Equation (54) implies that the importance of surface and rotational diffusion is determined by the ratios  $D_{\text{surf}}/D_{3d}$  and  $R^2 D_{\text{rot}}/D_{3d}$ . Recalling that  $D_{3d}$  is the sum of the cell and reactant translational diffusivities and assuming the Stokes–Einstein relation holds (as is done, for example, for rotational diffusion of *E. coli*; see pages 81–83 in [10]), we have

$$(55) \quad D_{3d} = \frac{k_B T}{6\pi\eta R_{\text{cell}}} + \frac{k_B T}{6\pi\eta R_{\text{reac}}}, \quad D_{\text{rot}} = \frac{k_B T}{8\pi\eta (R_{\text{cell}})^3},$$

where  $R_{\text{cell}}, R_{\text{reac}}$  are the radii of the cell and reactant,  $k_B$  is Boltzmann’s constant,  $T$  is temperature, and  $\eta$  is the viscosity of the extracellular medium. Noting that  $R = R_{\text{cell}} + R_{\text{reac}}$ , we have that (55) implies [12]

$$(56) \quad R^2 D_{\text{rot}}/D_{3d} = \frac{3}{4}(\rho + \rho^2), \quad \rho := R_{\text{reac}}/R_{\text{cell}}.$$

Equation (56) has two immediate consequences. First, if the reactant is small compared to the cell ( $\rho \ll 1$ ), then cell rotational diffusion only mildly increases reaction rates. Indeed, if  $\rho = 0.1$ , then (56) implies (ignoring receptor diffusion)

$$\lambda = \sqrt{1 + R^2 D_{\text{rot}}/D_{3d}} \approx 1.04.$$

Thus, rotational diffusion yields only a 4% increase in reaction rate. While small, we note that a 4% increase is comparable to a well-known correction to the reaction rate based on receptor competition [97] (see the section below for more details). Second, if the reactant is not much smaller than the cell, then rotational diffusion significantly increases reaction rates. To illustrate, if  $\rho = 1$ , then

$$\lambda = \sqrt{1 + R^2 D_{\text{rot}}/D_{3d}} \approx 1.58,$$

meaning rotational diffusion alone yields a 58% increase.

Moving to receptor diffusion, (55) implies

$$(57) \quad D_{\text{surf}}/D_{3d} = \chi D_{\text{surf}} R_{\text{cell}} \left( \frac{\rho}{1 + \rho} \right), \quad \chi := \frac{6\pi\eta}{k_B T}.$$

Now, diffusion coefficients of membrane-associated proteins are typically in the range  $D_{\text{surf}} \in [0.01, 0.5] \mu\text{m}^2/\text{s}$  [56, 87]. In addition, a typical cell radius is between  $R_{\text{cell}} = 0.35 \mu\text{m}$  (a small bacteria) and  $R_{\text{cell}} = 15 \mu\text{m}$  (a large mammalian cell). Hence, if we take  $\eta$  to be the viscosity of water and  $T = 293 \text{ K}$ , then (57) implies the typical range

$$(58) \quad 0.02 \left( \frac{\rho}{1 + \rho} \right) \leq D_{\text{surf}}/D_{3d} \leq 31 \left( \frac{\rho}{1 + \rho} \right).$$

The lower and upper bounds in (58) correspond, respectively, to  $D_{\text{surf}} = 0.01 \mu\text{m}^2/\text{s}$ ,  $R_{\text{cell}} = 0.35 \mu\text{m}$  and  $D_{\text{surf}} = 0.5 \mu\text{m}^2/\text{s}$ ,  $R_{\text{cell}} = 15 \mu\text{m}$ .

Equations (57)–(58) imply that if the reactant is not much smaller than the cell ( $\rho \approx 1$  or  $\rho > 1$ ), then receptor diffusion significantly increases reaction rates for large cells and/or very mobile receptors. For example, if  $\rho = 1$ ,  $D_{\text{surf}} = 0.5 \mu\text{m}^2/\text{s}$ , and  $R_{\text{cell}} = 15 \mu\text{m}$ , then (ignoring rotation)

$$\lambda = \sqrt{1 + D_{\text{surf}}/D_{3\text{d}}} \approx 4.06,$$

meaning receptor diffusion alone quadruples the reaction rate. Furthermore, even if we decrease the relative size to  $\rho = 0.1$  (implying the cell volume is 1000 times greater than the reactant volume), it follows that  $\lambda \approx 1.96$  and thus receptor diffusion almost doubles the reaction rate. Of course, (57) also implies that the effect of receptor diffusion decreases as we reduce  $D_{\text{surf}}$ ,  $R_{\text{cell}}$ , and/or  $\rho$ .

**6.2. Chemoreception and bacteriophage adsorption.** We now apply our results to some biological scenarios. In the case of chemoreception, the reactant is much smaller than a cell and, thus, (56) and (57) imply that both rotational diffusion and receptor diffusion have almost no impact on reaction rates. For example, in the case of bacteria sensing amino acids, we have  $\rho < 0.005$ , in which case (56)–(57) with  $R_{\text{cell}} = 0.35 \mu\text{m}$  and  $D_{\text{surf}} = 0.5 \mu\text{m}^2/\text{s}$  yield  $\lambda < 1.004$ .

In contrast, receptor and rotational diffusion have a stronger impact on bacterial cells adsorbing bacteriophages since bacteriophages are closer in size to bacteria. For example, if we consider *E. coli* adsorbing bacteriophage T4 and set  $R_{\text{cell}} = 0.35 \mu\text{m}$ ,  $R_{\text{reac}} = 0.1 \mu\text{m}$  [94], and  $D_{\text{surf}} = 0.5 \mu\text{m}^2/\text{s}$ , then  $R^2 D_{\text{rot}}/D_{3\text{d}} \approx 0.28$ ,  $D_{\text{surf}}/D_{3\text{d}} \approx 0.16$ , and  $\lambda \approx 1.20$ .

**6.3. Comparison to Zwanzig correction [97].** In the subsections above, we found that the impact of rotational and surface diffusion on association rates in certain biological scenarios can range from less than one percent to tens of percentage points. To put these results in context, we compare them to a well-known correction to the Berg and Purcell rate due to Zwanzig [97].

In [69], Northrup compared the Berg and Purcell [11] approximation  $J_{\text{bp}} = J_{\text{max}} \frac{\varepsilon N}{\varepsilon N + \pi}$  to Brownian dynamics simulations and found that  $J_{\text{bp}}$  underestimated the flux by approximately 5% for  $N = 256$  and  $\varepsilon = 0.0628$ . Motivated by this discrepancy between numerical simulations and the formula  $J_{\text{bp}}$ , Zwanzig [97] postulated the following approximation to the flux based on an effective medium argument:

$$(59) \quad J_{\text{zw}} := J_{\text{max}} \frac{\varepsilon N}{\varepsilon N + (1-f)\pi}, \quad f := N\varepsilon^2/4.$$

The expression  $J_{\text{zw}}$  agreed with the simulations of [69] to experimental error [97].

How significant is this correction and how does the significance depend on parameters? The percentage difference between  $J_{\text{bp}}$  and  $J_{\text{zw}}$  is

$$(60) \quad \frac{J_{\text{zw}} - J_{\text{bp}}}{J_{\text{zw}}} = \frac{N\pi\varepsilon^2}{4N\varepsilon + 4\pi} \leq \lim_{N \rightarrow \infty} \frac{N\pi\varepsilon^2}{4N\varepsilon + 4\pi} = \varepsilon \frac{\pi}{4}.$$

For the choice  $\varepsilon = 0.0628$  taken in [69], this difference is  $\varepsilon\pi/4 \approx 0.05$ , which matches the 5% difference between  $J_{\text{bp}}$  and the simulations in [69]. As is apparent from (60), this difference vanishes as  $\varepsilon \rightarrow 0$ . Indeed, in Berg and Purcell's application to bacteriophage adsorption [11], they took  $\varepsilon = 0.0065$ , which implies that the percentage difference between  $J_{\text{bp}}$  and  $J_{\text{zw}}$  is at most one-half of one percentage point.

**7. Discussion.** In closing, we discuss our results in the context of prior work. Our result in (1) generalizes the Berg and Purcell [11] result in (7) to include receptor surface diffusion and rotational diffusion. A lot of very interesting work has been done to modify the Berg and Purcell result in (7) to account for details such as receptor competition and cell curvature [8, 9, 33, 39, 62, 68, 97]. Most of the prior work uses heuristic arguments and parameter fits to simulation data.

However, a systematic mathematical approach was recently developed in [62]. Indeed, our implementation of the method of matched asymptotic analysis was inspired by [62]. This asymptotic method has been successfully applied in a number of important works investigating diffusive search for small targets, including [29, 30, 32, 92, 93]. We note that while these previous works study random processes, the analysis is performed on a deterministic PDE describing a statistic of the process (typically a mean first passage time). In contrast, the present work analyzes a stochastic PDE.

We are not aware of any prior work that calculates how receptor surface diffusion influences rates of binding to extracellular reactants. Prior work that sought to incorporate cell rotational diffusion includes [12, 78, 85]. These works consider only a single receptor on the surface of the cell, and they typically study a resulting deterministic PDE boundary value problem by first applying a quasi-chemical [85] or related [78] approximation, then use separation of variables to obtain an infinite series solution, and finally take certain parameter limits to obtain tractable formulas from the infinite series. For example, formula (18a) in [12] implies that the flux into a single hole of radius  $\varepsilon R$  with  $\varepsilon \ll 1$  is (in our notation)

$$(61) \quad J_{\max} \sqrt{1 + D_{\text{rot}}/D_{3\text{d}}} \varepsilon / (2\sqrt{2}).$$

Hence, our result in (32) (with  $N = 1$ ,  $D_{\text{surf}} = 0$ ) corrects (61) by replacing  $1/(2\sqrt{2}) \approx 0.35$  by  $1/\pi \approx 0.32$ . Further, (36) generalizes (61) to include  $N \geq 1$  receptors that diffuse with diffusivity  $D_{\text{surf}} \geq 0$ .

Additional related work includes studies of diffusive search for stochastically gated targets [3, 21, 22, 24, 74], deterministically moving targets [19, 63, 64, 91], and diffusive targets [17, 18, 42, 43, 66, 73, 83, 90]. The study of diffusive search for diffusive targets originally arose in the physics literature [89] as a model of monopole-antimonopole annihilation in the early Universe, but applications to chemical kinetics and condensed matter physics have driven much of the subsequent development. In contrast to this previous work on diffusive targets, our work studies interdimensional reactions, as the reactants diffuse in three dimensions and the receptors diffuse in two dimensions. This interdimensionality also distinguishes our work from the well-studied two step “reduction of dimensionality” process, in which the reactant first nonspecifically adsorbs to the membrane and then undergoes two-dimensional diffusion to reach the receptor [1, 6, 7, 75, 76].

In addition, the model in the present work resembles several recent biological models involving the diffusion equation with stochastically switching boundary conditions [60, 23, 57]. These models have been applied to diverse biological applications, including volume neurotransmission [58, 59], insect respiration [60, 25], and intercellular signaling [20, 26]. In contrast to the present work, these previous models are *piecewise deterministic*. That is, these models evolve deterministically between the discrete times when the boundary conditions randomly change (the boundary conditions typically switch according to a Markov jump process). In the present work, however, the stochastic boundary conditions evolve continuously according to the SDEs in (11).

Finally, the present work could be extended to account for additional aspects of the membrane environment. For example, not only do receptors diffuse, but their diffusion coefficient can randomly fluctuate (sometimes due to being trapped in membrane subdomains such as lipid rafts [80, 65]). Two key examples are (i) LFA-1 receptors that alternate between fast and slow diffusive states [34, 81] and (ii) AMPA receptors on the postsynaptic membrane that alternate within seconds between rapid diffusive and stationary states [16]. To extend the present work to such heterogeneous diffusion, one could assume the receptor diffusivity fluctuates between discrete states, as in [27, 28, 61].

An additional extension would be to receptors that must wait a refractory or “recharge” time between successive bindings [46, 47]. That is, while most models assume that receptors can continuously bind extracellular reactants, in many systems the receptors are temporarily inactive following each binding. For example, synaptic receptors on neural membranes undergo a transitory conformational change after binding a neurotransmitter, and during this time the receptor is unable to bind additional neurotransmitters. A similar scenario occurs, for example, in experiments where neuroactive compounds are released into extracellular space and bind to receptors on astrocytes [86]. Such a recharge time was recently shown to have a drastic effect in other contexts [46, 47], and it would be interesting to see how it affects the association rates studied in the present work.

**Acknowledgments.** The authors gratefully acknowledge many helpful conversations with James P. Keener. The support and resources from the Center for High Performance Computing at the University of Utah are gratefully acknowledged.

#### REFERENCES

- [1] G. ADAM AND M. DELBRÜCK, *Reduction of dimensionality in biological diffusion processes*, in Structural Chemistry and Molecular Biology, Freeman, San Francisco, 1968, pp. 198–215.
- [2] N. AGMON AND A. SZABO, *Theory of reversible diffusion-influenced reactions*, J. Chem. Phys., 92 (1990), pp. 5270–5284.
- [3] H. AMMARI, J. GARNIER, H. KANG, H. LEE, AND K. SÖLNA, *The mean escape time for a narrow escape problem with multiple switching gates*, Multiscale Model Simul, 9 (2011), pp. 817–833.
- [4] S. S. ANDREWS AND D. BRAY, *Stochastic simulation of chemical reactions with spatial resolution and single molecule detail*, Phys. Biol., 1 (2004), pp. 137–151, <https://doi.org/10.1088/1478-3967/1/3/001>.
- [5] G. AQUINO, N. S. WINGREEN, AND R. G. ENDRES, *Know the single-receptor sensing limit? Think again*, J. Stat. Phys., 162 (2016), pp. 1353–1364.
- [6] O. BENICHO, D. GREBENKOV, P. LEVITZ, C. LOVERDO, AND R. VOITURIEZ, *Optimal reaction time for surface-mediated diffusion*, Phys. Rev. Lett., 105 (2010), 150606, <https://doi.org/10.1103/PhysRevLett.105.150606>.
- [7] O. BENICHO, D. S. GREBENKOV, P. E. LEVITZ, C. LOVERDO, AND R. VOITURIEZ, *Mean first-passage time of surface-mediated diffusion in spherical domains*, J. Stat. Phys., 142 (2011), pp. 657–685, <https://doi.org/10.1007/s10955-011-0138-6>.
- [8] A. BEREZHKOVSII, Y. MAKHOVSKII, M. MONINE, V. ZITSERMAN, AND S. SHVARTSMAN, *Boundary homogenization for trapping by patchy surfaces*, J. Chem. Phys., 121 (2004), pp. 11390–11394.
- [9] A. M. BEREZHKOVSII, M. I. MONINE, C. B. MURATOV, AND S. Y. SHVARTSMAN, *Homogenization of boundary conditions for surfaces with regular arrays of traps*, J. Chem. Phys., 124 (2006), 036103.
- [10] H. C. BERG, *Random Walks in Biology*, Princeton University Press, Princeton, NJ, 1993.
- [11] H. C. BERG AND E. M. PURCELL, *Physics of chemoreception*, Biophys. J., 20 (1977), pp. 193–219.
- [12] O. BERG, *Orientation constraints in diffusion-limited macromolecular association: The role of surface diffusion as a rate-enhancing mechanism*, Biophys. J., 47 (1985), pp. 1–14.

- [13] O. G. BERG AND P. H. VON HIPPEL, *Diffusion-controlled macromolecular interactions*, *Annu. Rev. Biophys.*, 14 (1985), pp. 131–158.
- [14] A. J. BERNOFF AND A. E. LINDSAY, *Numerical approximation of diffusive capture rates by planar and spherical surfaces with absorbing pores*, *SIAM J. Appl. Math.*, 78 (2018), pp. 266–290.
- [15] W. BIALEK AND S. SETAYESHGAR, *Physical limits to biochemical signaling*, *Proc. Natl. Acad. Sci. USA*, 102 (2005), pp. 10040–10045.
- [16] A. J. BORGENDORFF AND D. CHOQUET, *Regulation of AMPA receptor lateral movements*, *Nature*, 417 (2002), pp. 649–653.
- [17] M. BRAMSON AND J. L. LEBOWITZ, *Asymptotic behavior of densities in diffusion-dominated annihilation reactions*, *Phys. Rev. Lett.*, 61 (1988), pp. 2397–2400.
- [18] A. J. BRAY AND R. A. BLYTHE, *Exact asymptotics for one-dimensional diffusion with mobile traps*, *Phys. Rev. Lett.*, 89 (2002), 150601.
- [19] A. J. BRAY AND R. SMITH, *The survival probability of a diffusing particle constrained by two moving, absorbing boundaries*, *J. Phys. A*, 40 (2007), pp. F235–F242.
- [20] P. C. BRESSLOFF, *Diffusion in cells with stochastically gated gap junctions*, *SIAM J. Appl. Math.*, 76 (2016), pp. 1658–1682.
- [21] P. C. BRESSLOFF AND S. D. LAWLEY, *Escape from a potential well with a randomly switching boundary*, *J. Phys. A*, 48 (2015), 225001, <https://doi.org/10.1088/1751-8113/48/22/225001>.
- [22] P. C. BRESSLOFF AND S. D. LAWLEY, *Escape from subcellular domains with randomly switching boundaries*, *Multiscale Model Simul.*, 13 (2015), pp. 1420–1445.
- [23] P. C. BRESSLOFF AND S. D. LAWLEY, *Moment equations for a piecewise deterministic PDE*, *J. Phys. A*, 48 (2015), 105001, <https://doi.org/10.1088/1751-8113/48/10/105001>,
- [24] P. C. BRESSLOFF AND S. D. LAWLEY, *Stochastically gated diffusion-limited reactions for a small target in a bounded domain*, *Phys. Rev. E* (3), 92 (2015), 062117.
- [25] P. C. BRESSLOFF AND S. D. LAWLEY, *Diffusion on a tree with stochastically gated nodes*, *J. Phys. A*, 49 (2016), 245601.
- [26] P. C. BRESSLOFF AND S. D. LAWLEY, *Dynamically active compartments coupled by a stochastically-gated gap junction*, *J. Nonlinear Sci.*, 27 (2017), pp. 1487–1512.
- [27] P. C. BRESSLOFF AND S. D. LAWLEY, *Temporal disorder as a mechanism for spatially heterogeneous diffusion*, *Phys. Rev. E* (3), 95 (2017), 060101.
- [28] P. C. BRESSLOFF, S. D. LAWLEY, AND P. MURPHY, *Protein concentration gradients and switching diffusions*, *Phys. Rev. E* (3), 99 (2019), 032409.
- [29] A. F. CHEVIAKOV AND M. J. WARD, *Optimizing the principal eigenvalue of the laplacian in a sphere with interior traps*, *Math. Comput. Model*, 53 (2011), pp. 1394–1409, <https://doi.org/10.1016/j.mcm.2010.02.025>.
- [30] A. F. CHEVIAKOV, M. J. WARD, AND R. STRAUBE, *An asymptotic analysis of the mean first passage time for narrow escape problems: Part II: The sphere*, *Multiscale Model Simul.*, 8 (2010), pp. 836–870.
- [31] D. CHOQUET AND A. TRILLER, *The dynamic synapse*, *Neuron*, 80 (2013), pp. 691–703.
- [32] D. COOMBS, R. STRAUBE, AND M. WARD, *Diffusion on a sphere with localized traps: Mean first passage time, eigenvalue asymptotics, and Fekete points*, *SIAM J. Appl. Math.*, 70 (2009), pp. 302–332, <https://doi.org/10.1137/080733280>.
- [33] L. DAGDUG, M. VÁZQUEZ, A. BEREZHKOVSII, AND V. ZITSERMAN, *Boundary homogenization for a sphere with an absorbing cap of arbitrary size*, *J. Chem. Phys.*, 145 (2016), 214101.
- [34] R. DAS, C. W. CAIRO, AND D. COOMBS, *A hidden Markov model for single particle tracks quantifies dynamic interactions between LFA-1 and the actin cytoskeleton*, *PLoS Comput. Biol.*, 5 (2009), e1000556.
- [35] C. DEQUIDT, L. DANGLLOT, P. ALBERTS, T. GALLI, D. CHOQUET, AND O. THOUMINE, *Fast turnover of L1 adhesions in neuronal growth cones involving both surface diffusion and exo/endocytosis of L1 molecules*, *Mol. Biol. Cell.*, 18 (2007), pp. 3131–3143.
- [36] D. B. DUSENBERY, *Spatial sensing of stimulus gradients can be superior to temporal sensing for free-swimming bacteria*, *Biophys. J.*, 74 (1998), pp. 2272–2277.
- [37] A. H. ELCOCK, D. SEPT, AND J. A. MCCAMMON, *Computer Simulation of Protein-Protein Interactions*, *J. Phys. Chem. B*, 105 (2001), pp. 1504–1518.
- [38] R. G. ENDRES AND N. S. WINGREEN, *Accuracy of Direct Gradient Sensing by Single Cells*, *Proc. Natl. Acad. Sci. USA*, 105 (2008), pp. 15749–15754.
- [39] C. EUN, *Effect of surface curvature on diffusion-limited reactions on a curved surface*, *J. Chem. Phys.*, 147 (2017), 184112.
- [40] V. FABRIKANT, *Applications of Potential Theory in Mechanics: A Selection of New Results*, *Math. Appl.* 51, Kluwer Academic, Dordrecht, The Netherlands, 1989.

- [41] S. FANCHER AND A. MUGLER, *Fundamental limits to collective concentration sensing in cell populations*, Phys. Rev. Lett., 118 (2017), 078101.
- [42] A. GABEL, S. MAJUMDAR, N. PANDURANGA, AND S. REDNER, *Can a lamb reach a haven before being eaten by diffusing lions?*, J. Stat. Mech. Theory Exp., 2012 (2012), P05011.
- [43] L. GIUGGIOLI, S. PÉREZ-BECKER, AND D. P. SANDERS, *Encounter times in overlapping domains: Application to epidemic spread in a population of territorial animals*, Phys. Rev. Lett., 110 (2013), 058103.
- [44] T. GREGOR, D. W. TANK, E. F. WIESCHAUS, AND W. BIALEK, *Probing the limits to positional information*, Cell, 130 (2007), pp. 153–164.
- [45] J. HALATEK AND E. FREY, *Highly canalized mind transfer and mine sequestration explain the origin of robust mincde-protein dynamics*, Cell Rep., 1 (2012), pp. 741–752.
- [46] G. HANDY, S. D. LAWLEY, AND A. BORISYUK, *Receptor recharge time drastically reduces the number of captured particles*, PLOS Comput. Biol., 14 (2018), e1006015.
- [47] G. HANDY, S. D. LAWLEY, AND A. BORISYUK, *Role of trap recharge time on the statistics of captured particles*, Phys. Rev. E (3), 99 (2019), 022420.
- [48] D. HOLCMAN AND Z. SCHUSS, *Time scale of diffusion in molecular and cellular biology*, J. Phys. A, 47 (2014), 173001.
- [49] M. HOWARD, *How to build a robust intracellular concentration gradient*, Trends Cell. Biol., 22 (2012), pp. 311–317.
- [50] I. KARATZAS AND S. SHREVE, *Brownian Motion and Stochastic Calculus*, Grad Tests in Math. 113, Springer, New York, 1988.
- [51] R. A. KERR, H. LEVINE, T. J. SEJNOWSKI, AND W.-J. RAPPEL, *Division accuracy in a stochastic model of min oscillations in escherichia coli*, Proc. Natl. Acad. Sci. USA, 103 (2006), pp. 347–352.
- [52] B. N. KHOLODENKO, *Cell-signalling dynamics in time and space*, Nat. Rev. Mol. Cell Biol., 7 (2006), pp. 165–176.
- [53] P. E. KLOEDEN AND E. PLATEN, *Numerical Solution of Stochastic Differential Equations*, coor. ed., Springer, Berlin, 1992.
- [54] Y. Y. KUTTNER, N. KOZER, E. SEGAL, G. SCHREIBER, AND G. HARAN, *Separating the contribution of translational and rotational diffusion to protein association*, J. Amer. Chem. Soc., 127 (2005), pp. 15138–15144.
- [55] T. LAGACHE AND D. HOLCMAN, *Extended narrow escape with many windows for analyzing viral entry into the cell nucleus*, J. Stat. Phys., 166 (2017), pp. 244–266.
- [56] D. A. LAUFFENBURGER AND J. LINDERMAN, *Receptors: Models for Binding, Trafficking, and Signaling*, Oxford University Press, New York, 1993.
- [57] S. D. LAWLEY, *Boundary value problems for statistics of diffusion in a randomly switching environment: PDE and SDE perspectives*, SIAM J. Appl. Dyn. Syst., 15 (2016), pp. 1410–1433.
- [58] S. D. LAWLEY, *A probabilistic analysis of volume transmission in the brain*, SIAM J. Appl. Math., 78 (2018), pp. 942–962.
- [59] S. D. LAWLEY, J. BEST, AND M. C. REED, *Neurotransmitter concentrations in the presence of neural switching in one dimension*, Discrete Contin. Dyn. Syst. Ser. B, 21 (2016), pp. 2255–2273.
- [60] S. D. LAWLEY, J. C. MATTINGLY, AND M. C. REED, *Stochastic switching in infinite dimensions with applications to random parabolic PDE*, SIAM J. Math. Anal., 47 (2015), pp. 3035–3063, <https://doi.org/10.1137/140976716>.
- [61] S. D. LAWLEY AND C. E. MILES, *Diffusive Search for Diffusing Targets with Fluctuating Diffusivity and Gating*, submitted, 2018.
- [62] A. E. LINDSAY, A. J. BERNOFF, AND M. J. WARD, *First passage statistics for the capture of a Brownian particle by a structured spherical target with multiple surface traps*, Multiscale Model Simul., 15 (2017), pp. 74–109.
- [63] A. E. LINDSAY, T. KOLOKOLNIKOV, AND J. C. TZOU, *Narrow escape problem with a mixed trap and the effect of orientation*, Phys. Rev. E (3), 91 (2015), 032111, <https://doi.org/10.1103/PhysRevE.91.032111>.
- [64] A. E. LINDSAY, J. C. TZOU, AND T. KOLOKOLNIKOV, *Optimization of first passage times by multiple cooperating mobile traps*, Multiscale Model Simul., 15 (2017), pp. 920–947.
- [65] D. LINGWOOD AND K. SIMONS, *Lipid rafts as a membrane-organizing principle*, Science, 327 (2010), pp. 46–50.
- [66] V. MEHRA AND P. GRASSBERGER, *Trapping reaction with mobile traps*, Phys. Rev. E (3), 65 (2002), 050101.
- [67] A. MUGLER, A. LEVCHENKO, AND I. NEMENMAN, *Limits to the precision of gradient sensing with spatial communication and temporal integration*, Proc. Natl. Acad. Sci. USA, 113 (2016), pp. E689–E695.

- [68] C. B. MURATOV AND S. Y. SHVARTSMAN, *Boundary homogenization for periodic arrays of absorbers*, Multiscale Model Simul., 7 (2008), pp. 44–61.
- [69] S. H. NORTHRUP, *Diffusion-controlled ligand binding to multiple competing cell-bound receptors*, J. Phys. Chem., 92 (1988), pp. 5847–5850, <https://doi.org/10.1021/j100331a060>.
- [70] S. H. NORTHRUP, M. S. CURVIN, S. A. ALLISON, AND J. A. MCCAMMON, *Optimization of Brownian dynamics methods for diffusion-influenced rate constant calculations*, J. Chem. Phys., 84 (1986), pp. 2196–2203, <https://doi.org/10.1063/1.450381>.
- [71] S. H. NORTHRUP AND H. P. ERICKSON, *Kinetics of protein-protein association explained by Brownian dynamics computer simulation.*, Proc. Natl. Acad. Sci. USA, 89 (1992), pp. 3338–3342.
- [72] N. RAPPAPORT AND N. BARKAI, *Disentangling signaling gradients generated by equivalent sources*, J. Biol. Phys., 38 (2012), pp. 267–278.
- [73] S. REDNER AND P. KRAPIVSKY, *Capture of the lamb: Diffusing predators seeking a diffusing prey*, Amer. J. Phys., 67 (1999), pp. 1277–1283.
- [74] J. REINGRUBER AND D. HOLCMAN, *Gated narrow escape time for molecular signaling*, Phys. Rev. Lett., 103 (2009), 148102.
- [75] J.-F. RUPPRECHT, O. BENICHO, D. S. GREBENKOV, AND R. VOITURIEZ, *Exact mean exit time for surface-mediated diffusion*, Phys. Rev. E (3), 86 (2012), 041135, <https://doi.org/10.1103/PhysRevE.86.041135>.
- [76] J.-F. RUPPRECHT, O. BENICHO, D. S. GREBENKOV, AND R. VOITURIEZ, *Kinetics of active surface-mediated diffusion in spherically symmetric domains*, J. Stat. Phys., 147 (2012), pp. 891–918, <https://doi.org/10.1007/s10955-012-0496-8>.
- [77] M. J. SAXTON, *Lateral Diffusion of Lipids and Proteins*, in Membrane Permeability, Current Topics Membranes 48, Academic Press, San Diego, CA, 1999, pp. 229–282.
- [78] D. SHOUP, G. LIPARI, AND A. SZABO, *Diffusion-controlled bimolecular reaction rates: The effect of rotational diffusion and orientation constraints*, Biophys. J., 36 (1981), pp. 697–714.
- [79] D. SHOUP AND A. SZABO, *Role of diffusion in ligand binding to macromolecules and cell-bound receptors*, Biophys. J., 40 (1982), pp. 33–39.
- [80] K. SIMONS AND D. TOOMRE, *Lipid rafts and signal transduction*, Nat. Rev. Mol. Cell. Biol., 1 (2000), pp. 31–39.
- [81] P. J. SLATOR, C. W. CAIRO, AND N. J. BURROUGHS, *Detection of diffusion heterogeneity in single particle tracking trajectories using a hidden Markov model with measurement noise propagation*, PLoS One, 10 (2015), e0140759.
- [82] M. SMOLUCHOWSKI, *Grundriß der koagulationskinetik kolloider lösungen*, Kolloid Z., 21 (1917), pp. 98–104.
- [83] I. SOKOLOV, H. SCHNÖRER, AND A. BLUMEN, *Diffusion-controlled reaction  $A + B \rightarrow 0$  in one dimension: The role of particle mobilities and the diffusion-equation approach*, Phys. Rev. A (3), 44 (1991), pp. 2388–2393.
- [84] K. SOLC AND W. STOCKMAYER, *Kinetics of diffusion-controlled reaction between chemically asymmetric molecules. I. General theory*, J. Chem. Phys., 54 (1971), pp. 2981–2988.
- [85] K. ŠOLC AND W. STOCKMAYER, *Kinetics of diffusion-controlled reaction between chemically asymmetric molecules. II. Approximate steady-state solution*, Int. J. Chem. Kinet., 5 (1973), pp. 733–752.
- [86] M. TAHERI, G. HANDY, A. BORISYUK, AND J. A. WHITE, *Diversity of evoked astrocyte  $Ca^{2+}$  dynamics quantified through experimental measurements and mathematical modeling*, Front. Syst. Neurosci., 11 (2017), 00079.
- [87] O. THOUMINE, E. SAINT-MICHEL, C. DEQUIDT, J. FALK, R. RUDGE, T. GALLI, C. FAIVRE-SARRAILH, AND D. CHOQUET, *Weak effect of membrane diffusion on the rate of receptor accumulation at adhesive contacts*, Biophys. J., 89 (2005), pp. L40–L42.
- [88] G. TKAČIK AND W. BIALEK, *Diffusion, dimensionality, and noise in transcriptional regulation*, Phys. Rev. E (3), 79 (2009), 051901.
- [89] D. TOUSSAINT AND F. WILCZEK, *Particle-antiparticle annihilation in diffusive motion*, J. Chem. Phys., 78 (1983), pp. 2642–2647.
- [90] J. TZOU, S. XIE, AND T. KOLOKOLNIKOV, *First-passage times, mobile traps, and Hopf bifurcations*, Phys. Rev. E (3), 90 (2014), 062138.
- [91] J. C. TZOU AND T. KOLOKOLNIKOV, *Mean first passage time for a small rotating trap inside a reflective disk*, Multiscale Model Simul., 13 (2015), pp. 231–255, <https://doi.org/10.1137/140968604>.
- [92] M. J. WARD, W. D. HESHAW, AND J. B. KELLER, *Summing logarithmic expansions for singularly perturbed eigenvalue problems*, SIAM J. Appl. Math., 53 (1993), pp. 799–828.
- [93] M. J. WARD AND J. B. KELLER, *Strong localized perturbations of eigenvalue problems*, SIAM J. Appl. Math., 53 (1993), pp. 770–798.

- [94] M. YAP AND M. ROSSMANN, *Structure and function of bacteriophage T4*, *Future Microbiol.*, 9 (2014), pp. 1319–1327.
- [95] H.-X. ZHOU, *Kinetics of diffusion-influenced reactions studied by Brownian dynamics*, *J. Phys. Chem.*, 94 (1990), pp. 8794–8800.
- [96] H.-X. ZHOU, *Brownian dynamics study of the influences of electrostatic interaction and diffusion on protein-protein association kinetics*, *Biophys. J.*, 64 (1993), pp. 1711–1726.
- [97] R. ZWANZIG, *Diffusion-controlled ligand binding to spheres partially covered by receptors: An effective medium treatment*, *Proc. Natl. Acad. Sci. USA*, 87 (1990), pp. 5856–5857.